INTERFACE

Research

Author for correspondence:
Pawel R. Golyski
e-mail: pgolyski3@gatech.edu

THE ROYAL SOCIETY
PUBLISHING

Which lower limb joints compensate for destabilizing energy during walking in humans?

Pawel R. Golyski[1,2] and Gregory S. Sawicki[1,2,3,4]

[1]Parker H. Petit Institute for Bioengineering and Biosciences, [2]George W. Woodruff School of Mechanical Engineering, [3]Institute for Robotics and Intelligent Machines, and [4]School of Biological Sciences, Georgia Institute of Technology, Atlanta, GA, USA

iD PRG, 0000-0001-9844-2859

Current approaches to investigating stabilizing responses during locomotion lack measures that both directly relate to perturbation demands and are shared across different levels of description (i.e. joints and legs). Here, we investigated whether mechanical energy could serve as a 'common currency' during treadmill walking with transient unilateral belt accelerations. We hypothesized that by delivering perturbations in either early or late stance, we could elicit net negative or positive work, respectively, from the perturbed leg at the leg/treadmill interface, which would dictate the net demand at the overall leg level. We further hypothesized that of the lower limb joints, the ankle would best reflect changes in overall leg work. On average across all seven participants and 222 perturbations, we found early stance perturbations elicited no change in net work performed by the perturbed leg on the treadmill, but net positive work by the overall leg, which did not support our hypotheses. Conversely, late stance perturbations partially supported our hypotheses by eliciting positive work at the leg/treadmill interface, but no change in net work by the overall leg. In support of our final hypothesis, changes in perturbed ankle work, in addition to contralateral knee work, best reflected changes in overall leg work.

1. Introduction

Falls remain a major public health problem. In the United States alone, one in four adults over 65-year-old fall at least once a year, which results in over 25,000 deaths annually and $31 billion in annual direct healthcare costs [1–3]. In the workplace, falls caused 16% of fatal work-related injuries in 2019, with 68% of fall-related injuries occurring in individuals between 35 and 64 years old [4,5]. In both younger and older adults, falls occur more often during walking than any other locomotor task, with external disturbances such as slips and trips being the predominant perceived cause of falls [6,7]. Although responses to external perturbations have been extensively studied at the overall leg (e.g. foot placement), joints, and muscles (e.g. [8–17]), relating these different levels of description remains difficult. Two obstacles to such analyses are (i) variables used to characterize responses are generally not measured using a 'common currency' that can be easily related across different levels and (ii) the explicit, quantifiable demand imposed by the perturbation is unknown. In this work, we aimed to overcome these obstacles by using a split-belt treadmill to deliver destabilizing perturbations using transient changes in belt speed that imposed quantifiable energetic demands on the legs that could be related to changes in work at the joints. We anticipate this analysis will serve as an initial step in describing stabilizing responses at multiple levels using mechanical energetics.

The mechanical power of each leg during walking, with respect to a fixed global reference frame and assuming massless legs, can be estimated using

the individual limbs method [18], which quantifies the mechanical energy flowing between the ground and the centre of mass (COM). During overground walking, the mechanical power of each leg is the dot product of its corresponding ground reaction force (GRF) and COM velocity. No power flows between each leg and the ground because the velocity of the ground is 0, thus $\boldsymbol{F}_{\text{Leg}} \cdot \boldsymbol{v}_{\text{ground}} = 0$, where $\boldsymbol{F}_{\text{Leg}}$ is equal and opposite to the GRF. However, for treadmill walking, this is no longer the case; with respect to a fixed global reference frame, each belt is moving, so the power flowing from each leg to its corresponding belt is $\boldsymbol{F}_{\text{Leg}} \cdot \boldsymbol{v}_{\text{belt}}$. Thus, in the case of treadmill walking, the mechanical power of each leg is the sum of the power flowing from the leg to the treadmill belt and the leg to the COM [19].

During level ground treadmill walking with both belts of a split-belt treadmill moving at the same constant speed, the net work of each leg on the COM is zero on average over a stride. Further, with both belts moving at the same speed, since the average anteroposterior force must be zero over a stride (otherwise the COM would accelerate relative to the treadmill), each leg performs zero net mechanical work on its corresponding belt. Therefore, in this condition, the net work performed by each leg must be zero on average [20]. However, in either non-steady conditions or when belts of a split-belt treadmill are moving at different speeds, the previous assumptions no longer hold, and a treadmill can elicit an energetic demand on the leg over a stride. In this study, we leveraged this concept and designed perturbations intended to elicit a change in net work over a stride by a leg (i.e. generation or dissipation). Specifically, since leg force is directed anteriorly in early stance and posteriorly in late stance, by increasing the posterior velocity of a belt, our first hypothesis (H1) was that net negative work would be performed by the perturbed leg on the treadmill over a stride with an early stance perturbation, while net positive work would be performed with a late stance perturbation (figure 1). Our second hypothesis (H2) was that such changes in net work at the leg/treadmill interface relative to an unperturbed stride would be reflected at the level of overall leg work, since the treadmill environment limits large fluctuations in the COM velocity and thus also the mechanical power exchanged between each leg and the COM ($\boldsymbol{F}_{\text{GRF}} \cdot \boldsymbol{v}_{\text{COM}}$).

While no previous work has investigated the mechanical energetics of transient unilateral treadmill speed perturbations during walking, there are numerous experimental contexts that elicit an energetic demand on the legs during locomotion by changing the required amount of work that the legs perform on the COM. Examples include increasing or decreasing the slope of the ground relative to level [21–25], accelerating or decelerating [26,27] and falling into a hole [28,29]. In general, relative to level ground, walking on an incline results in a shift to more positive work and power at the hip joint [21–24], while walking on a decline results in more negative work and power at the knee joint [22–24]. However, in the case of speed changes and ground height perturbations, changes in ankle work and power best reflect the overall demand on the leg [26–30]. Since our perturbations were more similar to speed changes than slope changes, our third hypothesis (H3) was that changes in net leg work over a stride resulting from the perturbation would primarily be reflected by changes in net work at the ankle joint.

2. Methods

2.1. Experimental protocol

Seven young, healthy individuals (five males, two females, mean (s.d.): 25 (2) years, 178.5 (12.1) cm stature, 72.7 (13.3) kg) walked on an instrumented split-belt treadmill (CAREN; Motek, Netherlands). Following an unperturbed 5 min acclimation period at 1.25 m s^{-1} [31], transient unilateral belt accelerations were delivered during walking. Each perturbation was targeted to either early or late stance and either the left or right leg. Each timing/leg pairing was repeated 10 times (i.e. 2 legs × 2 timings × 10 repetitions = 40 perturbations per participant). The order of perturbations was randomized, with 30–40 steps between perturbations to ensure the perturbation was unexpected and the participant had returned to steady-state walking [32]. The perturbation algorithm is fully described elsewhere [33] and used real-time kinematic data to estimate the gait phase during walking. Perturbations consisted of a brief (mean duration: 340 ms, 32.9% perturbed gait cycle) increase in belt speed from 1.25 to 2.5 m s^{-1} (figure 1b). All participants provided informed consent as approved by the local Institutional Review Board.

2.2. Data acquisition

Three-dimensional forces from the instrumented treadmill were sampled at 2000 Hz and treadmill belt velocities were logged at approximately 70 Hz. Sixty-seven reflective markers (modified Human Body Model 2; [34]) were placed on the bony landmarks and major body segments (head, hands, forearms, upper arms, torso, pelvis, thighs, shanks, and feet) of each participant. A 10-camera motion capture system (Vicon; Oxford, UK) collected three-dimensional marker trajectories at 200 Hz. For each participant, a static trial was used to scale an individualized version of the generic full-body musculoskeletal model developed by Rajagopal and colleagues (37 degrees of freedom, 22 rigid bodies; [35]) in OpenSim v. 4.0 [36]. Trials where participants crossed over the belts, as determined by manual inspection, were removed from the analysis, leaving 222 successful trials.

2.3. Leg mechanical energetics

To calculate a 'ground truth' estimate of the overall mechanical powers of each leg, we used a modified version of the individual limbs method [18,19,37]. This 'corrected' overall leg power (as opposed to summing lower limb joint powers) was the sum of (i) the power flowing from each leg to the treadmill, (ii) the power flowing from each leg to the COM, and (iii) the peripheral powers of the leg segments (thigh, shank, and foot) relative to the COM. The power from the leg to the treadmill was calculated as the dot product of the force from each leg on the ground (equal and opposite to the GRF) with the velocity of the respective treadmill belt. The power from each leg to the COM was calculated as the dot product of each GRF and the velocity of the whole-body COM. Whole-body COM kinematics were calculated using the scaled musculoskeletal models and the OpenSim Body Kinematics tool. This kinematic COM estimate was selected instead of estimates based on the GRF [18–20] because GRF-based estimates of COM velocity solve for integration constants assuming steady-state behaviour over multiple strides, but such integration constants may not be valid during perturbed strides. The peripheral power of the leg segments was calculated by summing the time derivative of the rotational and translational components of kinetic energy [37–39].

2.4. Joint mechanical energetics

Joint-level powers were calculated as the product of joint angular velocities and joint moments. Joint angular velocities were calculated as the time derivative of joint angles produced using the
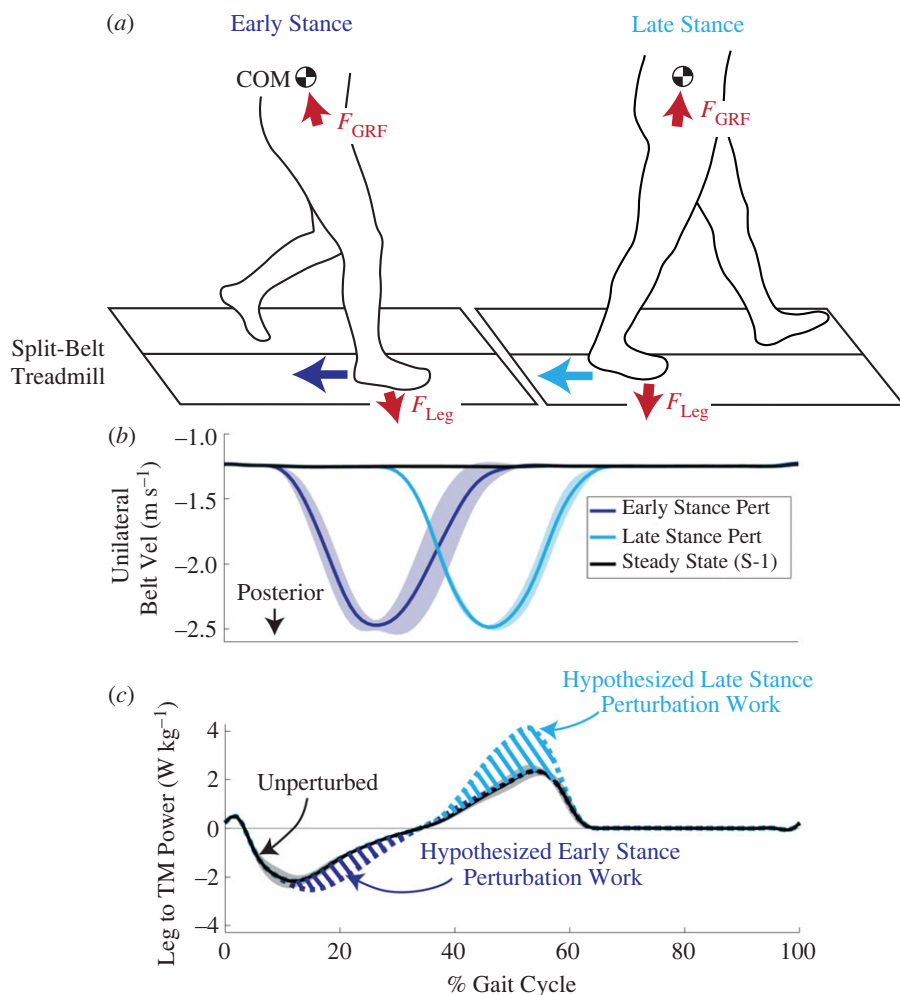
Figure 1. Perturbation overview. (*a*) Perturbation design. In early stance perturbations, since the leg force is anterior and treadmill velocity is posterior, this results in the leg performing negative work on the belt. In late stance, when leg force is posterior and treadmill velocity is posterior, the leg performs positive work on the belt. (*b*) Unilateral belt velocity traces show across-subject ensemble averages. Shaded regions represent ±1 s.d. (*c*) Hypothesized changes in power flowing from the leg to the treadmill relative to steady state, with early stance perturbations eliciting negative power (e.g. dissipation) and late stance perturbations eliciting positive power (e.g. generation).

OpenSim inverse kinematics tool. Joint moments were calculated with the OpenSim inverse dynamics tool using both the joint angles and bilateral GRFs applied to the calcanei of the scaled models. Joint kinematics and kinetics were low-pass filtered using fourth-order zero-phase Butterworth filters at 6 and 15 Hz, respectively. Strides were segmented using a 30 N threshold applied to vertical GRFs. To calculate summed joint power, joint powers about each available degree of freedom were summed (ankle plantar/dorsiflexion, knee flexion/extension, hip flexion/extension, hip ab/adduction, and hip external/internal rotation). The metatarsophalangeal (MTP) and subtalar joints of the models were locked in all analyses, thereby assuming the foot was a rigid body. To estimate leg power most accurately from joint power, six degrees of freedom joint powers and a deformable segment model for the foot are preferred [37,40–42], but such calculations are not compatible with the model-based OpenSim analysis that constrains joints to behave within physiological bounds. Sagittal plane joint angles and moments are not explicitly discussed in this work but are included in the electronic supplementary material (electronic supplementary material, figures S1 and S2, respectively). Mechanical work at the levels of the joints and legs was calculated using the trapezoidal integration of powers with respect to time.

2.5. Statistical analysis

All statistical analyses were performed in Matlab R2019b (Mathworks, Natick, MA, USA). Continuous outcome measures (i.e. gait cycle normalized profiles of power, force, velocity, etc.) of the early and late stance perturbation conditions were compared to steady-state profiles using statistical parametric mapping to perform paired *t*-tests [43]. This method evaluates the probability that smooth random curves would produce differences as large as those observed in the data and avoids the need to correct for multiple comparisons based on the number of data points in the traces. While we reported all statistical differences, readers should note that since the perturbations altered stride times and all profiles were normalized to the gait cycle, this produced some small phase shifts between perturbed and steady-state traces. As a result, some statistical differences were found between curves during periods of low variance and/or high slope which we did not interpret as being meaningful. For discrete outcome measures (i.e. mechanical work), a conventional paired *t*-test was used to compare the two perturbation conditions to steady-state levels. For H3, linear regressions were used to relate changes in corrected leg work with changes in ankle, knee, and hip work. For these regressions, changes in leg and joint work were calculated relative to steady-state strides (i.e. the work of stride S + N—work of stride S-1). Significance was concluded for *p*-values ≤ 0.05.

3. Results

3.1. H1—effect of perturbation timing on work performed by the perturbed leg on the treadmill

Both early and late stance perturbations elicited significant deviations in velocity, anteroposterior leg force and power
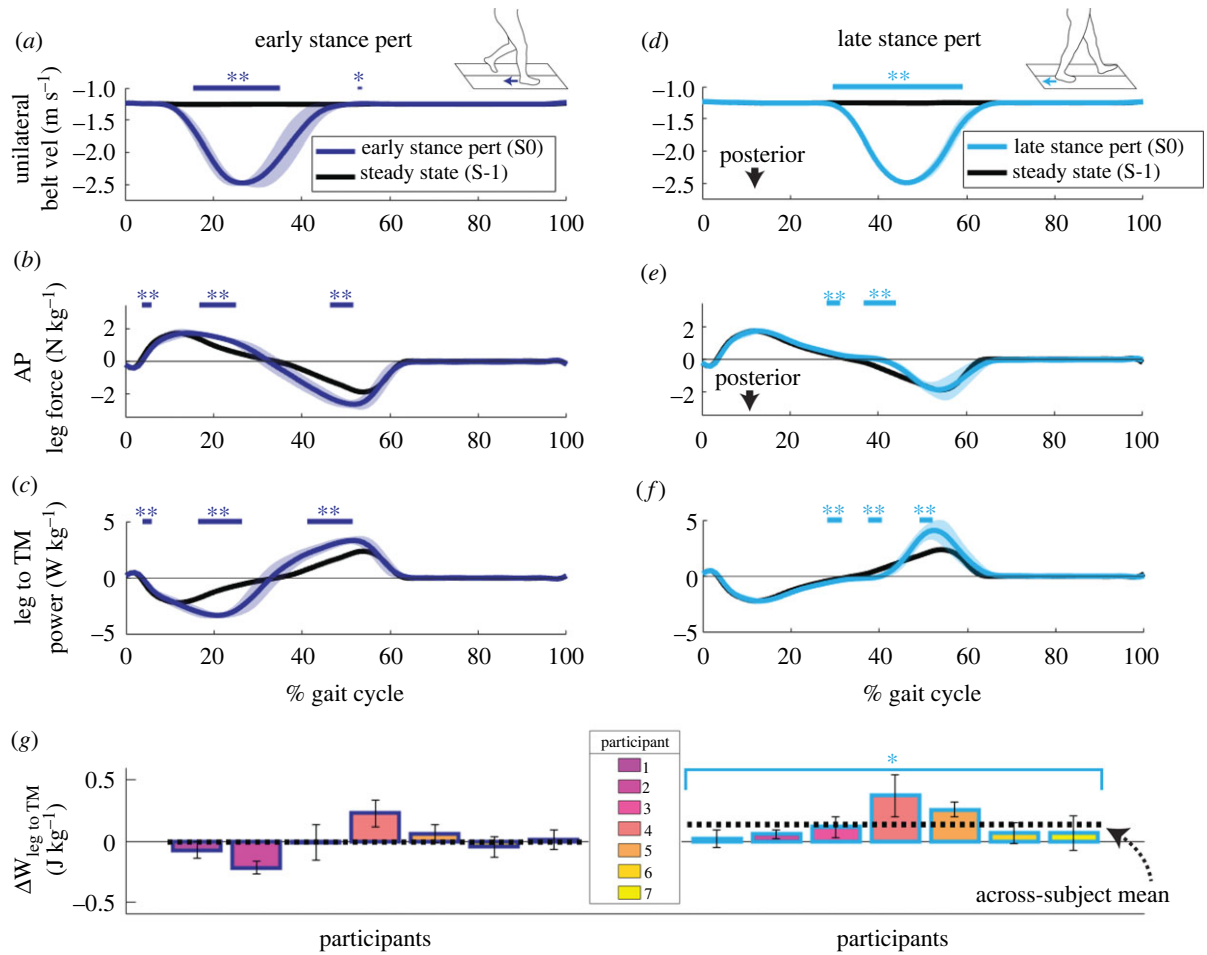
Figure 2. Results addressing H1 that early/late stance perturbations would elicit net negative/positive work, respectively, performed by the perturbed leg on the treadmill. Across-subject ensemble average (*a*,*d*) unilateral belt velocity traces, (*b*,*e*) anteroposterior forces exerted by the perturbed leg on the treadmill belt, and (*c*,*f*) power flowing from the leg to the treadmill belt. Instances when curves significantly deviated from steady state (S-1) are identified with thick horizontal lines and double asterisk (**) for $p < 0.001$ and thin horizontal lines and asterisk (*) for $p < 0.05$. (*g*) Power flowing from the perturbed leg to the treadmill was integrated in time to calculate the work contribution over the perturbed stride (S0). These values were subtracted from their respective measurements during steady-state strides (S-1) to quantify the changes in mechanical work at the leg/treadmill interface because of the perturbation. Statistical outcomes represent results of paired t-tests comparing work between the S0 versus S-1 strides. * = $p < 0.05$. Shaded regions (*a*–*f*) and error bars (*g*) represent ±1 s.d. See electronic supplementary material, figure S3 for three-dimensional leg and GRFs.

flowing from the leg to the treadmill on the perturbed side, relative to steady state (figure 2).

For early stance perturbations, the increased posterior velocity ($p < 0.001$; figure 2*a*) resulted in a larger anterior leg force before midstance ($p < 0.001$; figure 2*b*) and a larger posterior leg force in late stance ($p < 0.001$). The increased anterior leg force in early stance coupled with increased posterior velocity resulted in increased negative power flowing from the perturbed leg to the treadmill belt in early stance ($p < 0.001$; figure 2*c*), as we hypothesized. However, the increased posterior force in late stance also resulted in increased positive power flowing from the leg to the treadmill ($p < 0.001$). There was no significant difference in the net work performed by the perturbed leg on the treadmill over the stride relative to steady state ($p = 0.912$; figure 2*g*).

Late stance perturbations increased posterior velocity ($p < 0.001$; figure 2*d*), but had a limited effect on anteroposterior leg force, aside from a shift to more anteriorly directed force at approximately 40% of the gait cycle ($p < 0.001$; figure 2*e*). As hypothesized, there was significantly increased positive power flowing from the leg to the treadmill in late stance ($p < 0.001$; figure 2*f*), which resulted in a significant increase in net work performed by the perturbed leg on the treadmill over the stride relative to steady state ($p = 0.033$; figure 2*g*).

3.2. H2—effect of perturbation timing on overall corrected leg work

All three components of overall corrected leg power were influenced by each of the perturbation timings (figure 3). For early stance perturbations, significantly less negative power flowed from the perturbed leg to the COM in late stance ($p < 0.001$; figure 3*a*(i)), which resulted in net positive work being performed by the leg on the COM over the perturbed stride relative to steady state ($p < 0.001$, figure 3*c*, top row). Significantly more positive peripheral COM power was found in early stance ($p < 0.001$), and more negative peripheral COM power was found at the end of swing ($p = 0.005$). These peripheral COM power changes, in addition to changes that did not reach significance in late stance, resulted in no net change in peripheral COM work relative to steady state ($p = 0.170$). Since there was no change in work performed by the perturbed leg on the treadmill (see §3.1), combining all components of corrected leg work, we found there was net positive work performed by the overall leg relative to steady state ($p = 0.037$), in contrast with our hypothesis that there would be net negative work.

For late stance perturbations, significantly more negative power flowed from the perturbed leg to the COM in late stance ($p < 0.001$; figure 3*a*(ii)), which resulted in net negative
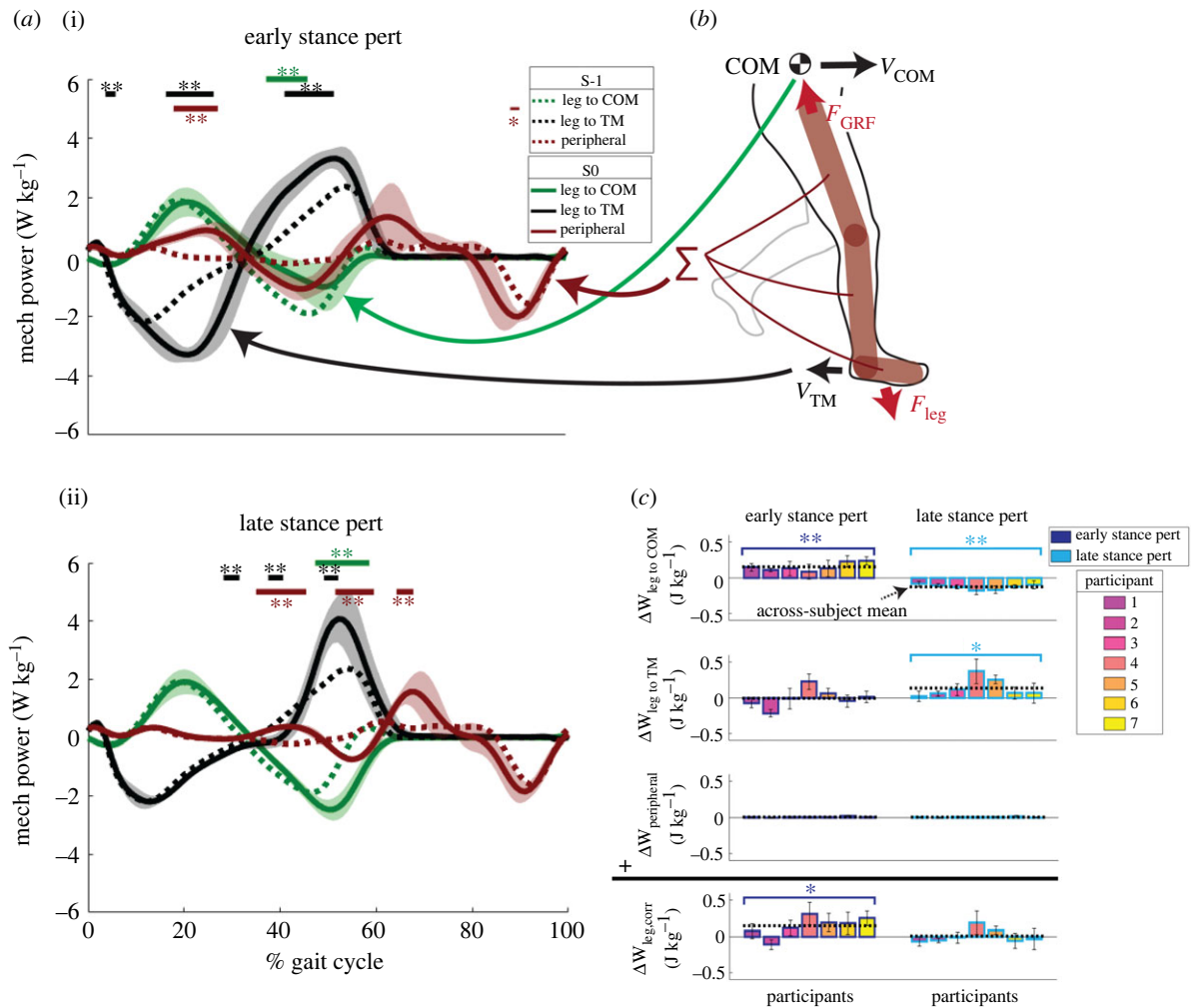
Figure 3. Results addressing H2 that early/late stance perturbations would elicit net negative/positive work, respectively, performed by the *overall leg* stemming from demands at the leg/treadmill interface. (*a*) Leg mechanical power breakdown for early stance (i) and late stance (ii) perturbations on the ipsilateral leg during the perturbed stride (S0, solid lines) and the unperturbed stride (S-1, dotted lines). For each perturbation timing, across-subject ensemble averages of the contributions to corrected individual leg power are shown (i.e. mechanical power flowing from the leg to the COM, power flowing from the leg to the treadmill and peripheral power of leg segments moving relative to the COM, all relative to a fixed laboratory frame). Shaded regions represent ±1 s.d. Instances when curves significantly deviated from steady state (S-1) are identified with thick horizontal lines and double asterisk (**) for $p < 0.001$ and thin horizontal lines and asterisk (*) for $p < 0.05$. (*b*) Graphical representation of contributions to corrected leg power. See §2.3 and 2.4 for a description of power calculations. (*c*) Contributions to corrected leg power were integrated in time to calculate the work contributions over the perturbed stride (S0). These values were subtracted from their respective measurements during steady-state strides (S-1) to quantify the changes in mechanical work of these contributions because of the perturbation. Error bars represent ±1 s.d. Statistical outcomes represent results of paired t-tests comparing work between the S0 versus S-1 strides. *$p < 0.05$, **$p < 0.001$.

work being performed by the leg on the COM over the perturbed stride relative to steady state ($p < 0.001$, figure 3c, top row). Although there were significant deviations in peripheral COM power in late stance ($p < 0.001$), as was the case for early stance perturbations, these changes were cancelled to result in no change in net peripheral COM work relative to steady state ($p = 0.291$). Altogether, the net positive work performed by the leg on the treadmill (see §3.1) cancelled with the net negative work performed by the leg on the COM to result in no net change in overall leg work relative to steady state for the late stance perturbations ($p = 0.848$). This was in contrast to our hypothesis that late stance perturbations would result in net positive work.

3.3. H3—relating overall leg to joint-level energetics
While across-subject analyses did not support H2, we found there was appreciable variability both within and among participants in the corrected leg work for both early and late

stance perturbations (figure 3c, bottom row). To investigate joint-level contributions to overall leg responses, we first assessed the agreement between corrected leg power and summed joint powers for the perturbed leg and stride (figure 4), then compared corrected leg work with individual joint work over the perturbed stride and first two recovery strides on both the perturbed (ipsilateral) and unperturbed (contralateral) legs (figure 5).

On the perturbed leg and stride, the agreement between corrected leg power and summed joint leg power was stronger for early stance perturbations than late stance perturbations ($R^2 = 0.82$ for early, $R^2 = 0.54$ for late). For both timings (thus likely not a result of the specific perturbations themselves), deviations in power curves were apparent just after the initial heel strike and in mid-swing. For early stance perturbations specifically, agreement significantly deviated at perturbation onset, with more negative corrected leg power than summed joint power ($p < 0.001$; figure 4a(i)). For late stance perturbations specifically, there
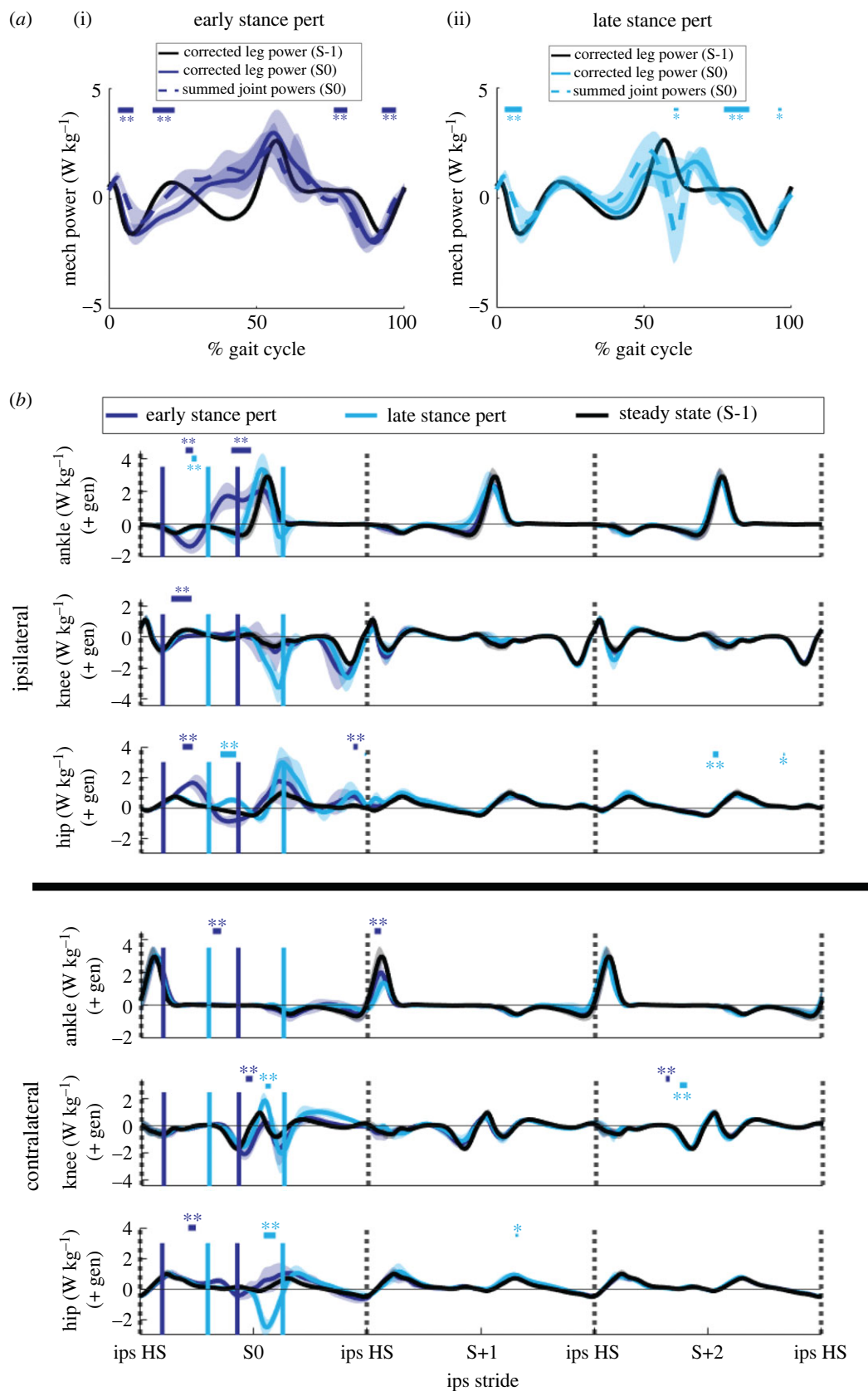
Figure 4. Results relating joint and leg powers for H3. (a) Comparison of corrected leg power and summed joint powers for early ((i), $R^2 = 0.82$) and late stance ((ii), $R^2 = 0.54$) perturbations. Instances when summed joint and corrected leg power curves significantly deviated are identified with thick horizontal lines and double asterisk (**) for $p < 0.001$ and thin horizontal lines and asterisk (*) for $p < 0.05$. (b) Sagittal plane lower limb joint mechanical powers averaged across subjects and normalized to the percentage of the gait cycle. Instances when curves significantly deviated from steady state (S-1) are identified with thick horizontal lines and double asterisk (**) for $p < 0.001$ and thin horizontal lines and asterisk (*) for $p < 0.05$. Shaded areas represent ±1 s.d. Solid vertical lines indicate the average start and end times of the perturbations. 'Steady State' strides were the strides preceding the perturbed stride (S-1).

was significantly more negative power during push-off for the summed joint power than the corrected leg power ($p = 0.006$; figure 4a(ii)).

The largest changes in joint powers from steady state generally occurred during the perturbed stride (figure 4b). Early stance perturbations elicited more negative power followed
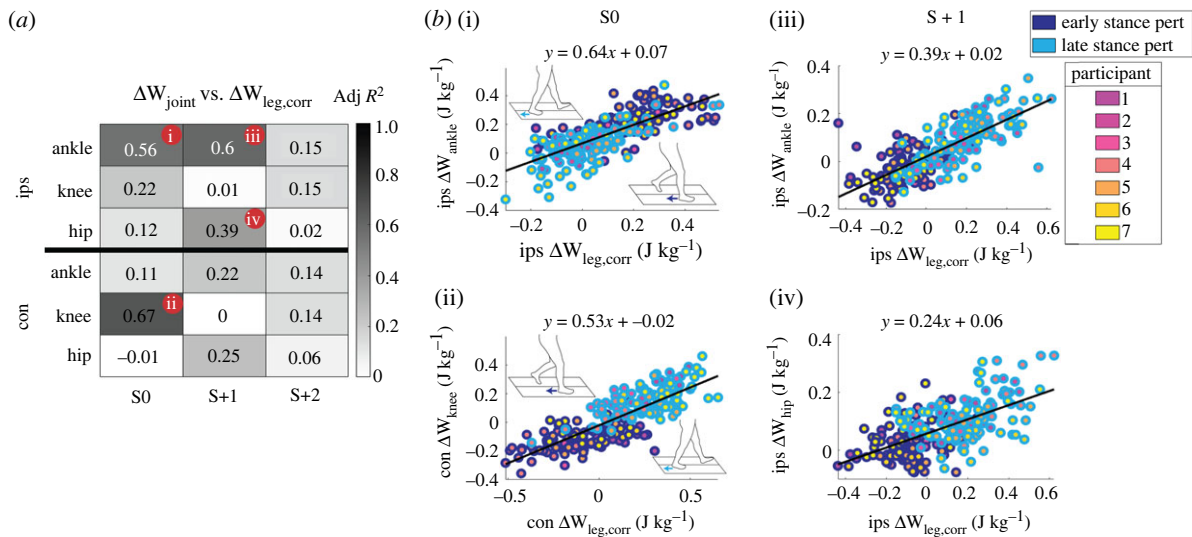
Figure 5. Results relating joint and corrected leg work for H3. (a) Adjusted R^2 values for linear regressions between differences in joint work over a stride from steady state and differences in corrected leg work over a stride from steady state (S-1) across all 222 perturbations. (b) (i–iv) Scatter plots for joint/stride with the highest adjusted R^2 values.

by a greater duration of positive power at the ipsilateral ankle ($p < 0.001$), in addition to more positive power during midstance at the ipsilateral hip ($p < 0.001$). On the contralateral side, early stance perturbations elicited more negative power at the knee at the end of contralateral swing ($p < 0.001$). Late stance perturbations elicited more negative power at the ipsilateral knee and positive power at the ipsilateral hip in late stance, although these deviations did not reach significance. On the contralateral side, late stance perturbations elicited increased positive power at the knee ($p < 0.001$) and negative power at the hip ($p < 0.001$) during the contralateral loading response. For both early and late stance perturbations, there was less positive push-off power at the ankle on the first recovery stride ($p < 0.001$).

Relating individual joint work with corrected leg work indicated that on the perturbed stride, changes in ipsilateral ankle ($R^2 = 0.56$, figure 5(i)) and contralateral knee work ($R^2 = 0.67$, figure 5(ii)) best reflect changes in overall leg work as a result of the perturbation. On the first recovery stride, changes in ipsilateral ankle ($R^2 = 0.60$, figure 5(iii)) and hip work ($R^2 = 0.39$, figure 5(iv)) best reflected changes in corrected leg work.

4. Discussion

The main objective of this work was to relate overall leg and joint-level responses to destabilizing perturbations during walking using mechanical energetics. We used a split-belt treadmill to elicit transient mechanical energetic demands on the legs during walking and investigated which joints best reflected those demands. Our first hypothesis (H1) was that unilateral belt accelerations delivered in early or late stance would elicit net negative or positive work, respectively, from the perturbed leg at the leg/treadmill interface over a stride. Our data supported this hypothesis for late stance perturbations, but not for early stance perturbations. In the case of early stance perturbations, while more negative power was elicited from the leg at the leg/treadmill interface in early stance, the posterior

movement of the leg caused by the perturbation led to a more posteriorly directed leg force ([10], figure 2b). This posterior leg force resulted in more positive power flowing from the leg to the treadmill in late stance, and no change in net work over a stride by the perturbed leg on the treadmill belt. Thus, future work seeking to specifically elicit net negative work at the leg/treadmill interface over a stride should consider decelerating the targeted treadmill belt during late stance, thereby avoiding unexpected compensations to the perturbation.

Our second hypothesis (H2) was that changes in net work at the leg/treadmill interface over the perturbed stride would be reflected by changes in overall leg work. Our data did not support this hypothesis for either early or late stance perturbations. For early stance perturbations, which we initially hypothesized would elicit net negative work from the perturbed leg, we found net *positive* work was generated by the leg. This occurred due to the combined effect of the net zero work performed by the leg on the treadmill coupled with less negative COM work in late stance. We attribute this decrease in negative COM work to a combination of (i) offloading of the perturbed leg around toe-off resulting in decreased negative COM power (electronic supplementary material, figure S3) and (ii) the perturbed leg accelerating the COM forward, as evidenced by an increased anteroposterior component of leg power (electronic supplementary material, figure S4). For late stance perturbations, which we initially hypothesized would elicit net positive work from the perturbed leg, we found no net change in work performed by the leg. In this case, the increased positive work performed by the leg on the treadmill was offset by the increased negative work of the leg on the COM in late stance. Increased negative COM power occurred despite the perturbed leg being offloaded, indicating the COM experienced a larger downward velocity around toe-off during late stance perturbations (electronic supplementary material, figures S3 and S4). Since the COM during double support is closer to the ground with faster walking speeds [44], this downward velocity may stem from the increased COM velocity caused by the perturbation coinciding with late stance. An additional observation from the responses in

overall leg work was the diversity of responses, particularly *among* participants, which was driven primarily by differences in work at the leg/treadmill interface (figure 3*c*). This emphasizes the need for subject specificity in devices or interventions designed to improve perturbation response.

Our third hypothesis (H3) was that changes in net ankle work elicited by perturbations would best reflect changes in net overall leg work. Although the energetic demands imposed on the perturbed leg were not as hypothesized, our perturbations nevertheless elicited both generation and dissipation, providing a rich dataset to relate leg- and joint-level mechanical energetics. Our hypothesized contribution by the ankle was supported on the perturbed stride and first recovery stride on the perturbed leg, with a large percentage of the change in work of the perturbed leg being accounted for by the ankle alone (64 and 39% for the perturbed and first recovery stride, respectively). While the importance of the ankle joint in generating mechanical power during steady-state walking [21,22,45] and acceleration [26,27,30] has been established, our findings demonstrate that the ankle also plays an important role in mediating transient demands, in agreement with previous studies of human hopping [28]. However, in contrast with the perturbed leg, for the contralateral leg, the knee joint best reflected changes in leg work during the perturbed stride. While previous studies have identified the knee joint as a major contributor during tasks requiring dissipation, such as deceleration and drop landings [27,46], we found that the knee additionally reflected the mechanical work of the leg when generation was required. This could be explained by the knee being a major source of collisional and rebound work in early/midstance, as opposed to the ankle, which primarily contributes later in stance through push-off [37]. Further, previous work that disrupted ankle push-off found that both positive and negative knee energetics were significantly altered [47].

One technical limitation of this work was that joint power contributions did not fully account for corrected overall leg power, particularly during late stance perturbations. Since both the corrected leg power and summed joint power were calculated using the same GRFs, and the respective curves for the contralateral leg on the perturbed stride were in better agreement ($R^2 = 0.90$ for early stance perturbations, 0.98 for late stance perturbations), the discrepancy between them is likely related to the centre of pressure deviations altering moments during the perturbation. These deviations could be caused by acceleration or deceleration of the treadmill rollers inducing a moment and altering the centre of pressure [48,49]. Additionally, modelling assumptions could propagate moment and power discrepancies from the foot to other joints. Future work seeking to overcome modelling discrepancies could consider using six degrees of freedom-based inverse dynamics [37,40,41] versus musculoskeletal model-based inverse dynamics, or a musculoskeletal model with free MTP and subtalar joints. Another important limitation of this work was the use of correlations to relate the

joint and limb levels. While this approach suggests which joints reflect demands at the leg level, it does not establish whether those joint-level responses *cause* changes at the leg level. Future work may further investigate the energetic link between joint- and leg-level responses by perturbing joint energetics and observing leg-level responses, perhaps using wearable robots that inject/extract mechanical energy [50–52]. Further, future studies may also use other types of perturbations, such as belt decelerations [13,16,53], external pushes [54] or obstacles [8], to determine whether these findings generalize to other unstable contexts. Lastly, inverse dynamics can only quantify net joint powers and does not capture the contributions of muscle–tendon units to energy exchanges across either side of a joint (e.g. coactivation [55]) and between joints (e.g. biarticular muscle–tendon units [56]), which could be explored using musculoskeletal simulations, electromyography coupled with *in vivo* imaging approaches and animal models [57–59].

In conclusion, we have demonstrated that a framework using mechanical energetics can be used to investigate joint-level contributions to the energetic demand imposed by a transient treadmill-based perturbation during human walking. We found that the net energetic demand on the perturbed leg during the perturbed stride varied depending on the timing of the perturbation, with changes in net leg work stemming from both changes in power flowing from the leg to the COM and from the leg to the treadmill. The varied energetic demands imposed across timings revealed that the ankle best reflected changes in energetics of the perturbed leg on the perturbed and first recovery strides, while the contralateral knee best reflected changes in energetics of the contralateral leg during the perturbed stride. We anticipate this work will serve as an initial step in using mechanical energetics to relate different levels of musculoskeletal description in unstable contexts.

References

1. Hartholt KA, Lee R, Burns ER, van Beeck EF. 2019 Mortality from falls among US adults aged 75 years or older, 2000–2016. *JAMA* **321**, 2131–2133. (doi:10.1001/jama.2019.4185)

2. Moreland B, Kakara R, Henry A. 2020 Trends in nonfatal falls and fall-related injuries among adults

aged ≥65 years—United States, 2012–2018. *MMWR Morb. Mortal. Wkly. Rep.* **69**, 875–881. (doi:10.15585/mmwr.mm6927a5)

3. Burns ER, Stevens JA, Lee R. 2016 The direct costs of fatal and non-fatal falls among older adults—United States. *J. Safety Res.* **58**, 99–103. (doi:10.1016/j.jsr.2016.05.001)

4. US Bureau of Labor Statistics. 2021 Injuries, illnesses, and fatalities program. See https://www.bls.gov/iif/.

5. Yeoh HT, Lockhart TE, Wu X. 2013 Non-fatal occupational falls on the same level. *Ergonomics* **56**, 153–165. (doi:10.1080/00140139.2012.746739)

6. Berg WP, Alessio HM, Mills EM, Tong C. 1997 Circumstances and consequences of falls in independent community-dwelling older adults. *Age Ageing* **26**, 261–268. (doi:10.1093/ageing/26.4.261)

7. Talbot LA, Musiol RJ, Witham EK, Metter EJ. 2005 Falls in young, middle-aged and older community dwelling adults: perceived cause, environmental factors and injury. *BMC Public Health* **5**, 1–9. (doi:10.1186/1471-2458-5-86)

8. King ST, Eveld ME, Martínez A, Zelik KE, Goldfarb M. 2019 A novel system for introducing precisely-controlled, unanticipated gait perturbations for the study of stumble recovery. *J. Neuroeng. Rehabil.* **16**, 1–17. (doi:10.1186/s12984-019-0527-7)

9. Grabiner MD, Koh TJ, Lundin TM, Jahnigen DW. 1993 Kinematics of recovery from a stumble. *J. Gerontol. Med. Sci.* **48**, M97–M102. (doi:10.1093/geronj/48.3.M97)

10. Debelle H, Harkness-Armstrong C, Hadwin K, Maganaris CN, O'Brien TD. 2020 Recovery from a forward falling slip: measurement of dynamic stability and strength requirements using a split-belt instrumented treadmill. *Front. Sports Act. Living* **2**, 1–13. (doi:10.3389/fspor.2020.00082)

11. Eng JJ, Winter DA, Patla AE. 1994 Strategies for recovery from a trip in early and late swing during human walking. *Exp. Brain Res.* **102**, 339–349. (doi:10.1007/BF00227520)

12. Schillings AM, van Wezel BMH, Mulder T, Duysens J. 2000 Muscular responses and movement strategies during stumbling over obstacles. *J. Neurophysiol.* **83**, 2093–2102. (doi:10.1152/jn.2000.83.4.2093)

13. Sloot LH, van den Noort JC, van der Krogt MM, Bruijn SM, Harlaar J. 2015 Can treadmill perturbations evoke stretch reflexes in the calf muscles? *PLoS ONE* **10**, e0144815. (doi:10.1371/journal.pone.0144815)

14. Pijnappels M, Bobbert MF, van Dieën JH. 2004 Contribution of the support limb in control of angular momentum after tripping. *J. Biomech.* **37**, 1811–1818. (doi:10.1016/j.jbiomech.2004.02.038)

15. Tang PF, Woollacott MH, Chong RKY. 1998 Control of reactive balance adjustments in perturbed human walking: roles of proximal and distal postural muscle activity. *Exp. Brain Res.* **119**, 141–152. (doi:10.1007/s002210050327)

16. Roeles S, Rowe PJ, Bruijn SM, Childs CR, Tarfali GD, Steenbrink F, Pijnappels M. 2018 Gait stability in response to platform, belt, and sensory perturbations in young and older adults. *Med. Biol. Eng. Comput.* **56**, 2325–2335. (doi:10.1007/s11517-018-1855-7)

17. Li J, Huang HJ. 2021 Small directional treadmill perturbations induce differential gait stability adaptation. *J. Neurophysiol.* **127**, 38–55. (doi:10.1152/jn.00091.2021)

18. Donelan JM, Kram R, Kuo AD. 2002 Simultaneous positive and negative external mechanical work in human walking. *J. Biomech.* **35**, 117–124. (doi:10.1016/S0021-9290(01)00169-5)

19. Selgrade BP, Thajchayapong M, Lee GE, Toney ME, Chang YH. 2017 Changes in mechanical work during neural adaptation to asymmetric locomotion. *J. Exp. Biol.* **220**, 2993–3000. (doi:10.1242/jeb.149450)

20. Sánchez N, Simha SN, Donelan JM, Finley JM. 2019 Taking advantage of external mechanical work to reduce metabolic cost: the mechanics and energetics of split-belt treadmill walking. *J. Physiol.* **597**, 4053–4068. (doi:10.1113/JP277725)

21. Montgomery JR, Grabowski AM. 2018 The contributions of ankle, knee and hip joint work to individual leg work change during uphill and downhill walking over a range of speeds. *R. Soc. Open Sci.* **5**, 180550. (doi:10.1098/rsos.180550)

22. Nuckols RW, Takahashi KZ, Farris DJ, Mizrachi S, Riemer R, Sawicki GS. 2020 Mechanics of walking and running up and downhill: a joint-level perspective to guide design of lower-limb exoskeletons. *PLoS ONE* **15**, 1–20. (doi:10.1371/journal.pone.0231996)

23. Alexander N, Strutzenberger G, Ameshofer LM, Schwameder H. 2017 Lower limb joint work and joint work contribution during downhill and uphill walking at different inclinations. *J. Biomech.* **61**, 75–80. (doi:10.1016/j.jbiomech.2017.07.001)

24. Lay AN, Hass CJ, Richard Nichols T, Gregor RJ. 2007 The effects of sloped surfaces on locomotion: an electromyographic analysis. *J. Biomech.* **40**, 1276–1285. (doi:10.1016/j.jbiomech.2006.05.023)

25. Roberts TJ, Belliveau RA. 2005 Sources of mechanical power for uphill running in humans. *J. Exp. Biol.* **208**, 1963–1970. (doi:10.1242/jeb.01555)

26. Schache AG, Lai AKM, Brown NAT, Crossley KM, Pandy MG. 2019 Lower-limb joint mechanics during maximum acceleration sprinting. *J. Exp. Biol.* **222**, jeb209460. (doi:10.1242/jeb.209460)

27. Qiao M, Jindrich DL. 2016 Leg joint function during walking acceleration and deceleration. *J. Biomech.* **49**, 66–72. (doi:10.1016/j.jbiomech.2015.11.022)

28. Dick TJM, Punith LK, Sawicki GS. 2019 Humans falling in holes: adaptations in lower-limb joint mechanics in response to a rapid change in substrate height during human hopping. *J. R. Soc. Interface* **16**, 20190292. (doi:10.1098/rsif.2019.0292)

29. Daley MA, Felix G, Biewener AA. 2007 Running stability is enhanced by a proximo-distal gradient in joint neuromechanical control. *J. Exp. Biol.* **210**, 383–394. (doi:10.1242/jeb.02668)

30. Farris DJ, Raiteri BJ. 2017 Modulation of leg joint function to produce emulated acceleration during walking and running in humans. *R. Soc. Open Sci.* **4**, 160901. (doi:10.1098/rsos.160901)

31. Zeni JA, Higginson JS. 2010 Gait parameters and stride-to-stride variability during familiarization to walking on a split-belt treadmill. *Clin. Biomech.* **25**, 383–386. (doi:10.1016/j.clinbiomech.2009.11.002)

32. Liu C, de Macedo L, Finley JM. 2018 Conservation of reactive stabilization strategies in the presence of step length asymmetries during walking. *Front. Hum. Neurosci.* **12**, 1–13. (doi:10.3389/fnhum.2018.00251)

33. Golyski PR, Vazquez E, Leestma JK, Sawicki GS. 2021 Onset timing of treadmill belt perturbations influences stability during walking. *J. Biomech.* **130**, 110800. (doi:10.1016/j.jbiomech.2021.110800)

34. van den Bogert AJ, Geijtenbeek T, Even-Zohar O, Steenbrink F, Hardin EC. 2013 A real-time system for biomechanical analysis of human movement and muscle function. *Med. Biol. Eng. Comput.* **51**, 1069–1077. (doi:10.1007/s11517-013-1076-z)

35. Rajagopal A, Dembia CL, DeMers MS, Delp DD, Hicks JL, Delp SL. 2016 Full-body musculoskeletal model for muscle-driven simulation of human gait. *IEEE Trans. Biomed. Eng.* **63**, 2068–2079. (doi:10.1109/TBME.2016.2586891)

36. Delp SL, Anderson FC, Arnold AS, Loan P, Habib A, John CT, Guendelman E, Thelen DG. 2007 OpenSim: open-source software to create and analyze dynamic simulations of movement. *IEEE Trans. Biomed. Eng.* **54**, 1940–1950. (doi:10.1109/TBME.2007.901024)

37. Zelik KE, Takahashi KZ, Sawicki GS. 2015 Six degree-of-freedom analysis of hip, knee, ankle and foot provides updated understanding of biomechanical work during human walking. *J. Exp. Biol.* **218**, 876–886. (doi:10.1242/jeb.115451)

38. Cavagna GA, Kaneko M. 1977 Mechanical work and efficiency in level walking and running. *J. Physiol.* **268**, 467–481. (doi:10.1113/jphysiol.1977.sp011866)

39. Willems PA, Cavagna GA, Heglund NC. 1995 External, internal and total work in human locomotion. *J. Exp. Biol.* **198**, 379–393. (doi:10.1242/jeb.198.2.379)

40. Duncan JA, Kowalk DL, Vaughan CL. 1997 Six degree of freedom joint power in stair climbing. *Gait Posture* **5**, 204–210. (doi:10.1016/S0966-6362(96)01086-7)

41. Buczek FL, Kepple TM, Siegel KL, Stanhope SJ. 1994 Translational and rotational joint power terms in a six degree-of-freedom model of the normal ankle complex. *J. Biomech.* **21**, 1447–1457. (doi:10.1016/0021-9290(94)90194-5)

42. Takahashi KZ, Kepple TM, Stanhope SJ. 2012 A unified deformable (UD) segment model for quantifying total power of anatomical and prosthetic below-knee structures during stance in gait. *J. Biomech.* **45**, 2662–2667. (doi:10.1016/j.jbiomech.2012.08.017)

43. Pataky TC, Vanrenterghem J, Robinson MA. 2015 Zero- vs. one-dimensional, parametric vs. non-parametric, and confidence interval vs. hypothesis testing procedures in one-dimensional biomechanical trajectory analysis. *J. Biomech.*

48, 1277–1285. (doi:10.1016/j.jbiomech.2015.02.051)

44. Orendurff MS, Segal AD, Klute GK, Berge JS, Rohr ES, Kadel NJ. 2004 The effect of walking speed on center of mass displacement. *J. Rehabil. Res. Dev.* **41**, 829–834. (doi:10.1682/JRRD.2003.10.0150)

45. Farris DJ, Sawicki GS. 2012 The mechanics and energetics of human walking and running: a joint level perspective. *J. R. Soc. Interface* **9**, 110–118. (doi:10.1098/rsif.2011.0182)

46. Yeow CH, Lee PVS, Goh JCH. 2010 Sagittal knee joint kinematics and energetics in response to different landing heights and techniques. *Knee* **17**, 127–131. (doi:10.1016/j.knee.2009.07.015)

47. Huang TWP, Shorter KA, Adamczyk PG, Kuo AD. 2015 Mechanical and energetic consequences of reduced ankle plantar-flexion in human walking. *J. Exp. Biol.* **218**, 3541–3550. (doi:10.1242/jeb.113910)

48. Hnat SK, van den Bogert AJ. 2014 Inertial compensation for belt acceleration in an instrumented treadmill. *J. Biomech.* **47**, 3758–3761. (doi:10.1016/j.jbiomech.2014.10.014)

49. Moore JK, Hnat SK, van den Bogert AJ. 2015 An elaborate data set on human gait and the effect of mechanical perturbations. *PeerJ* **3**, e918. (doi:10.7717/peerj.918)

50. Witte KA, Fiers P, Sheets-Singer AL, Collins SH. 2020 Improving the energy economy of human running with powered and unpowered ankle exoskeleton assistance. *Sci. Robot.* **5**, eaay9108. (doi:10.1126/scirobotics.aay9108)

51. Donelan JM, Li Q, Naing V, Hoffer JA, Weber DJ, Kuo AD. 2008 Biomechanical energy harvesting: generating electricity during walking with minimal user effort. *Science* **319**, 807–810. (doi:10.1126/science.1149860)

52. Shepertycky M, Burton S, Dickson A, Liu YF, Li Q. 2021 Removing energy with an exoskeleton reduces the metabolic cost of walking. *Science* **372**, 957–960. (doi:10.1126/science.aba9947)

53. Afschrift M, van Deursen R, de Groote F, Jonkers I. 2019 Increased use of stepping strategy in response to medio-lateral perturbations in the elderly relates to altered reactive tibialis anterior activity. *Gait Posture* **68**, 575–582. (doi:10.1016/j.gaitpost.2019.01.010)

54. Rong Tan G, Raitor M, Collins SH. 2020 Bump'em: an open-source, bump-emulation system for studying human balance and gait. In *2020 IEEE Int. Conf. on Robotics and Automation (ICRA) 31 May–31 August, 2020. Paris, France.* (doi:10.1109/ICRA40945.2020.9197105)

55. Abbott EM, Nezwek T, Schmitt D, Sawicki GS. 2019 Hurry up and get out of the way! Exploring the limits of muscle-based latch systems for power amplification. *Integr. Comp. Biol.* **59**, 1546–1558. (doi:10.1093/icb/icz141)

56. Iida F, Rummel J, Seyfarth A. 2008 Bipedal walking and running with spring-like biarticular muscles. *J. Biomech.* **41**, 656–667. (doi:10.1016/j.jbiomech.2007.09.033)

57. Dick TJM, Clemente CJ, Punith LK, Sawicki GS. 2021 Series elasticity facilitates safe plantar flexor muscle–tendon shock absorption during perturbed human hopping. *Proc. R. Soc. B* **288**, 20210201. (doi:10.1098/rspb.2021.0201)

58. Daley MA, Biewener AA. 2011 Leg muscles that mediate stability: mechanics and control of two distal extensor muscles during obstacle negotiation in the guinea fowl. *Phil. Trans. R. Soc. B* **366**, 1580–1591. (doi:10.1098/rstb.2010.0338)

59. Lai AKM, Biewener AA, Wakeling JM. 2019 Muscle-specific indices to characterise the functional behaviour of human lower-limb muscles during locomotion. *J. Biomech.* **89**, 134–138. (doi:10.1016/j.jbiomech.2019.04.027)